Svedberg Open
DISSEMINATION OF KNOWLEDGE

International Journal of Artificial Intelligence and Machine Learning

Publisher's Home Page: https://www.svedbergopen.com/

Research Paper Open Access

Technology, Roof Coverage, AND Export-Tariff Exposure IN Residential Rooftop Photovoltaics: A Bounded Re-Analysis OF Archived Simulation Results FOR A Single Dwelling IN A Hot Semi-Arid Indian Climate

Niraj Kathrani[1], Parwathi Pillai[2*]

[1]Department of Environmental Engineering, Swarrnim Institute of Technology, Swarrnim startup & Innovation University, Gandhinagar 382420, India.
[2]Department of Chemical Engineering, Swarrnim Institute of Technology, Swarrnim startup & Innovation University, Gandhinagar 382420, India.
[*]Corresponding Author, Email:
Parwathi.pillai@gmail.com, Parwathi.chemical@swarrnim.edu.in

Abstract
Design guidance for residential rooftop photovoltaics in India still treats roof coverage and module efficiency as interchangeable improvements, and screens projects on simple payback. This paper re-analyses archived EnergyPlus results for a two-storey dwelling in Ahmedabad (hot semi-arid, Köppen BSh), spanning a full factorial of three modules and four roof-coverage levels. Because the original model files are unavailable, every result is reported as a bounded range under two settlement regimes drawn from the governing Gujarat regulation and two capital-cost bases. Archived generation exceeded demand by 8 to 105 times, capping the billing-period set-off at 12.9% of output and exposing 87 to 100% of benefit to the export tariff, which accounted for 53% of variance in net present value against under 1% for the retail tariff. Coverage scaled generation almost in proportion to the area equipped, altering project size more than project quality. Under the archived area-proportional cost structure, module technology separated the configurations sharply, with levelised costs of ₹0.92 to 1.12 kWh^{-1} for crystalline silicon against ₹3.08 to 4.58 kWh^{-1} for the weakest thin-film option. Rebasing to national per-kilowatt benchmarks converged all twelve to ₹3.37 to 3.59 kWh^{-1} and left none viable at ₹2.00 kWh^{-1}, making roof area rather than unit cost the binding constraint. June to September carried 45.5% of demand but 23 to 27% of generation. A plausibility audit found implied capacities of 4.7 to 66.7 kW_p and mutually inconsistent module areas for configurations sharing one roof, so the study establishes a ranking rather than a business case.
Keywords: rooftop photovoltaics; building energy simulation; techno-economic assessment; net metering and export tariff; levelised cost of electricity; global sensitivity analysis.

Nomenclature

Symbol	Definition	Abbrev.	Definition
C_0	Initial capital cost (₹)	APPC	Average power purchase cost
E_g	Annual generation (kWh yr^{-1})	a-Si	Amorphous silicon
E_d	Annual electricity demand (kWh yr^{-1})	c-Si	Crystalline silicon
κ	Settlement regime indicator (–)	CAPEX	Capital expenditure
r	Real discount rate (–)	DPB	Discounted payback period
δ	Annual power degradation rate (–)	FF	First-floor roof
p_r, p_x	Retail and export tariff (₹ kWh^{-1})	GERC	Gujarat Electricity Regulatory Commission
N	Analysis period (yr)	GF	Ground-floor roof
S_i, S_{Ti}	First-order and total Sobol index (–)	IRR	Internal rate of return
ω, ρ	O&M and inverter-replacement fractions (–)	LCOE	Levelised cost of electricity
ε_g	Grid CO_2 emission factor (t MWh^{-1})	NPV	Net present value
Y_s	Specific yield (kWh kW_p^{-1} yr^{-1})	SPB	Simple payback period

1. Introduction

Buildings account for roughly a third of global final energy use and about 34% of energy-related carbon dioxide emissions, and sectoral emissions continue to rise (UNEP, 2025). The pressure is concentrated in rapidly urbanising economies where space cooling drives residential demand growth. Sherman et al. (2022) project the steepest increases in precisely those countries whose grids can least absorb sharp afternoon peaks, and metered Indian surveys show that adopting air conditioning restructures both the magnitude and the daily shape of household load (Ramapragada et al., 2022).

Rooftop photovoltaics addresses supply and demand at once. It displaces purchased electricity, and because the modules intercept radiation that would otherwise reach the roof, it also lowers the cooling load beneath. The thermal effect is established by measurement, with Dominguez et al. (2011) recording ceiling temperatures up to 2.5 K cooler beneath an array and Odeh and Pearling (2025) confirming the mechanism experimentally, and by simulation across climates (Kapsalis and Karamanis, 2015; Wang et al., 2020; Ma et al., 2023), including the Indian climate zones (Bhuvad and Udayraj, 2022). Physics-based building simulation suits such coupled problems because it resolves the enclosure and any attached generation within one heat balance (Crawley et al., 2001), and a methodological literature surrounds its use for design optimisation (Delgarm et al., 2016; Shi et al., 2016; Harkouss et al., 2018) and for treating uncertainty in its outputs (Chaturvedi et al., 2020; Chaturvedi and Rajasekar, 2022).

Whether such systems are worth building is a separate question, and two structural features govern the answer. The first is how generation divides between on-site set-off and export. Retail tariffs typically exceed export remuneration several-fold, so the same kilowatt-hour has very different value depending on where it goes. Luthander et al. (2015) identified self-consumption as the pivotal variable, and recent work confirms that the surplus-compensation rule can dominate prosumer returns (Aquila et al., 2024; Saez et al., 2024). The division depends on the settlement regime as much as on temporal coincidence, since net metering nets energy over a billing period whereas net billing settles generation and consumption separately. The second feature is the treatment of time. Simple payback, still the default screen in much applied work, ignores discounting, degradation and replacement, and can admit projects that a discounted appraisal rejects.

Indian residential studies have generally stopped short of both. Joshi and Pindoriya (2012) examined network impacts on a Gujarat feeder, Shukla et al. (2016) costed a standalone institutional system, P. Sharma et al. (2016) and Y. Sharma et al. (2019) applied analytical and HOMER-based treatments, and Behura et al. (2021) assessed a campus plant. These established feasibility, but the load is treated as exogenous, appraisal is deterministic, and the reported figure of merit is usually simple payback. The gap addressed here is therefore narrower than combining building and economic modelling, which is by now routine. It is the absence, for Indian residential rooftops, of a design comparison in which module technology and roof coverage are varied factorially against a physically simulated load, appraised on a discounted basis under the settlement regime that actually applies, and subjected to a global sensitivity analysis identifying which assumption governs the outcome.

This paper is a re-analysis rather than a new simulation study, and its scope is bounded accordingly. The energy quantities examined here were generated in an earlier EnergyPlus and DesignBuilder exercise whose model files, hourly outputs and array specifications are no longer available. Nothing in the archive can therefore be re-run, and several of its features cannot be checked at source. Rather than presenting archived outputs as validated model behaviour, the analysis treats them as a dataset of uncertain provenance: every economic result is reported as a range across two settlement regimes and two capital-cost bases, a plausibility audit tests the archived quantities against independent physical and regulatory reference points, and features that cannot be reconciled are reported as anomalies rather than as findings. Section 5.5 states what this design can and cannot support.

The objectives are: (i) to quantify separately the effects of module technology and roof coverage on annual yield and on the marginal cost of energy from each coverage increment; (ii) to characterise the seasonal coincidence of generation with a cooling-dominated load and the resulting division of benefit between set-off and export; (iii) to appraise all twelve configurations on discounted measures under both settlement regimes and both cost bases; (iv) to apportion the variance in project value using variance-based sensitivity indices; and (v) to audit the internal and external plausibility of the archived dataset itself.

The contribution is empirical and methodological. Empirically, the analysis shows for a low-demand, high-irradiance Indian setting that coverage and technology are not interchangeable levers, that the surplus-export tariff rather than the retail tariff or the capital subsidy governs value, and that generation is seasonally misaligned with cooling demand. Methodologically, it demonstrates that the apparent dominance of high-efficiency modules is contingent on how capital cost is attributed: under area-proportional costing efficiency decides unit cost, whereas under per-kilowatt benchmark costing unit costs converge and roof area becomes the binding constraint. It also illustrates how an archived simulation dataset can be interrogated for plausibility when the model itself has been lost. Section 2 positions the work, Section 3 describes the data and analysis, Section 4 reports results, Section 5 interprets them and states the limitations, and Section 6 concludes.

2. Related work and positioning

Three strands bear on this study. The first concerns the representation of photovoltaics inside building simulation. EnergyPlus attaches generators to surfaces whose heat balance it already solves (Crawley et al., 2001), and module behaviour follows the five-parameter equivalent one-diode formulation validated by De Soto et al. (2006), with plane-of-array irradiance obtained by standard transposition (Duffie and Beckman, 2013). Accuracy remains sensitive to how hourly insolation is decomposed into direct and diffuse components (An et al., 2020), so absolute yields from any single run are indicative rather than definitive. That caution applies with particular force to an archive that cannot be re-run.

The second strand concerns what photovoltaics does to the building. Beyond the measurements already cited, Zheng and Weng (2020) treated green roofs and modules as competing treatments of the same surface, Li et al. (2022) compared rooftop photovoltaics against radiative cooling, and Hoseinzadeh et al. (2021) extended the argument to façades. Ren et al. (2023) showed that realistic shading and rooftop availability change optimal packing decisions materially, which is a caution against models in which yield scales perfectly with area. The consistent finding is that the shading benefit is real but small relative to generation revenue.

The third strand concerns economics. Alhammami and An (2021) showed for Abu Dhabi that residential viability is created or destroyed by tariff design rather than resource quality. Pramadya and Kim (2024) found net metering and installation incentives not to be interchangeable, Aquila et al. (2024) formalised rolling credits against net billing, and Saez et al. (2024) quantified how surplus-compensation policy shapes Spanish rooftop economics. Kumar et al. (2024) provide compatible Indian evidence from the non-residential segment. Underpinning any long-horizon appraisal are field data on degradation: Jordan and Kurtz (2013) report a median near 0.5% per year with thin films degrading faster, Choi et al. (2018) document amorphous-silicon behaviour specifically, and Malvoni et al. (2020) assess a plant in a tropical semi-arid Indian environment, which also provides the specific-yield reference used in the plausibility audit below. For sensitivity analysis, variance-based decomposition is the established alternative to correlation-based attribution (Saltelli et al., 2010) and has been applied to photovoltaic techno-economics by Coppitters et al. (2019).

Table 1 positions this study along the five dimensions that determine what a study can conclude. Studies that model the building well tend to stop at energy, those that model economics well tend to treat the load as given, and few propagate uncertainty, report the settlement split that determines how each unit is valued, or audit their own inputs against external reference points.

Table 1. Positioning against closely related work. ✓ = addressed; ○ = partially addressed; – = not addressed.

Study	Setting	Load simulated	Technology × coverage	Discounted appraisal	Uncertainty propagated	Input plausibility audited
Joshi and Pindoriya (2012)	**Gujarat, India**	–	–	○	–	–
Shukla et al. (2016)	**Bhopal, India**	–	–	○	–	–
Behura et al. (2021)	**Vellore, India**	–	–	○	–	–
Alhammami and An (2021)	**Abu Dhabi, UAE**	–	–	✓	○	–
Bhuvad and Udayraj (2022)	**India, multi-zone**	✓	○	–	–	–
Ma et al. (2023)	**China**	✓	○	–	–	–
Aquila et al. (2024)	**Brazil**	–	–	✓	✓	–
Saez et al. (2024)	**Spain**	○	–	✓	○	–
Present study	**Ahmedabad, India**	○ (archived)	✓	✓	✓	✓

3. Data and methods

The workflow (Fig. 1) begins with an archived simulation dataset, subjects it to a plausibility audit, and then carries it through energy matching and a techno-economic assessment reported as bounded ranges. Each stage is described below. Quantities that could not be recovered from the archive are identified as such rather than substituted by assumption.

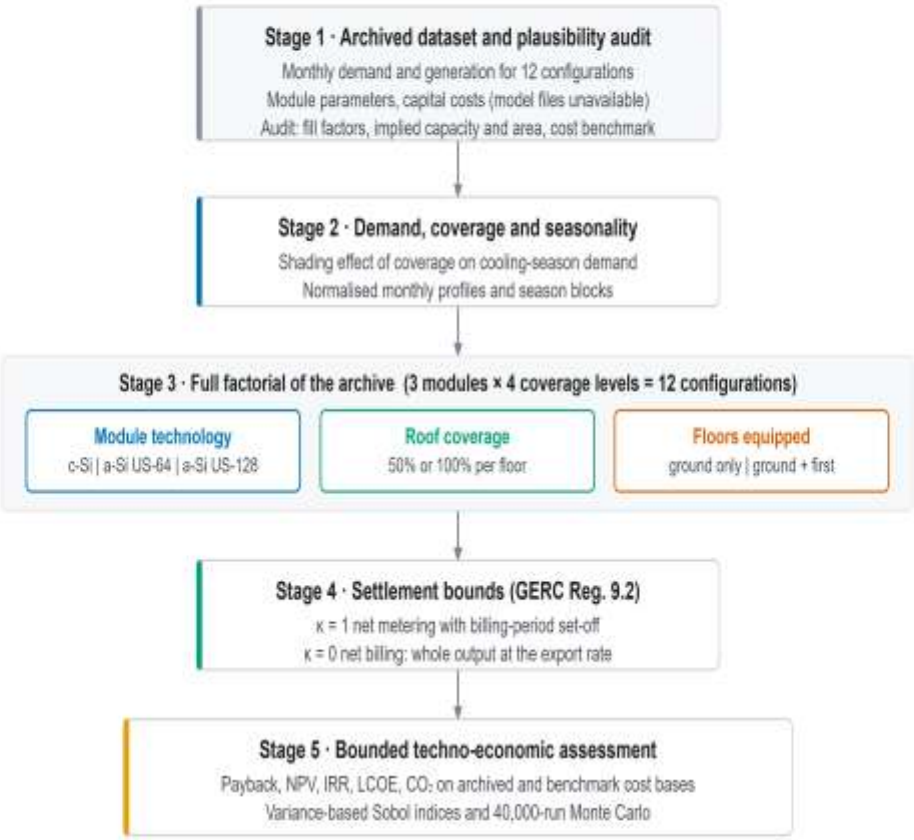

Fig. 1. Workflow of the re-analysis. Stage 1 audits the archived dataset against independent reference points; stages 3 to 5 report every economic result as a range across two settlement regimes and two capital-cost bases.

3.1 Provenance and status of the archived dataset

The energy quantities analysed here were produced in an earlier exercise using EnergyPlus with model geometry prepared in DesignBuilder. That exercise simulated a real two-storey detached residence in Ahmedabad, Gujarat (23.03° N, 72.58° E), in the hot semi-arid (BSh) Köppen–Geiger class and Climate Zone 2 of the National Building Code of India (Chaturvedi and Elangovan, 2023), using a typical-year EnergyPlus weather file for the city. What survives is a set of monthly and annual results: building electricity demand and photovoltaic generation for twelve rooftop configurations, together with the module parameters and capital costs reproduced in Tables 2 and 3.

The model files, the hourly output series, the array specifications and the software version records are not available, and the simulations cannot be re-run. Three consequences follow and are carried consistently through the paper. First, statements about the archived results are framed as observations about the dataset rather than as demonstrations of physical behaviour: the archived results indicate a given tendency, rather than the model showing it. Second, results that cannot be reconciled with the stated geometry or with the declared module technologies are reported as anomalies requiring confirmation, not as findings. Third, all economic outputs are presented as bounded ranges. Section 5.5 lists the disclosures a future study with access to the model would need to supply.

The archived description of the building is as follows. Opaque walls are fired-clay brick (density 1738 kg m^{-3}, specific heat 960.4 J kg^{-1} K^{-1}, conductivity 0.53 W m^{-1} K^{-1}); the roof is a 150 mm reinforced concrete slab with 10 mm expanded polystyrene; glazing is 6 mm clear single glass at a 15% window-to-wall ratio with 0.3 m overhangs. Three zones are mechanically cooled, two on the ground floor and one first-floor bedroom, each served by a 1.5-ton split unit with a 24 °C set point, while naturally ventilated zones use a 20 °C window-operation set point. Lighting and equipment are represented by a combined 6 W m^{-2} on the occupancy schedule. Simulations used the conduction-transfer-function heat balance at a one-hour time step over 8760 h.

Two features of that description cannot be reconciled and are reported rather than resolved. The cooling schedule is specified as 14:00 to 17:00 and 22:00 to 08:00, which spans thirteen hours per day although the archive describes it as nine. Cooling is stated to operate from April to August, yet the archived demand shows a September elevation (108 kWh against 38 kWh in October) that implies operation in September. This paper uses the archived demand as it stands and describes the operative period as April to September. The conditioned floor area, occupancy and infiltration assumptions and the equipment coefficient of performance were not recoverable, and no metered consumption was available, so the demand series is unvalidated and no NMBE or CV(RMSE) statistics are reported.

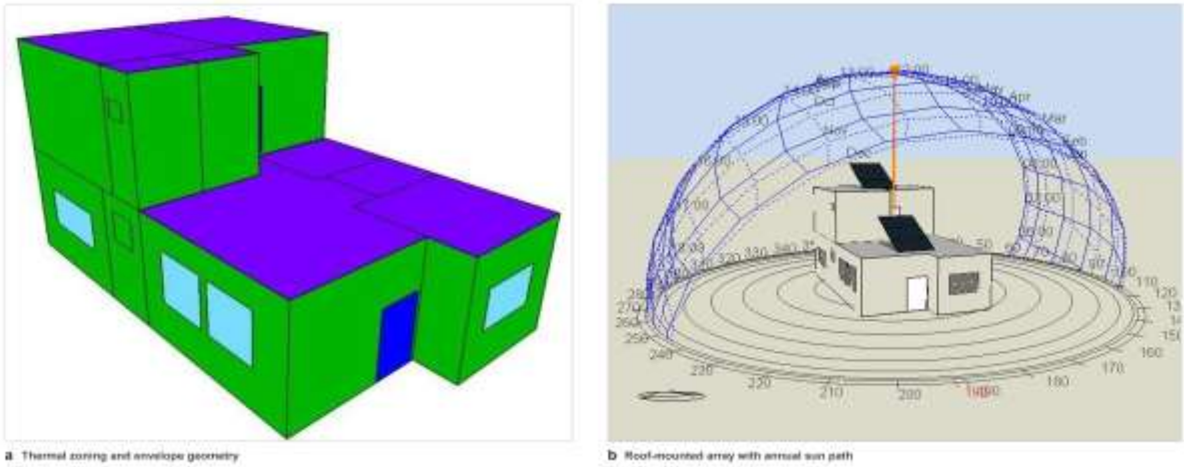

Fig. 2. Archived visualisations of the simulation model: (a) thermal zoning and envelope geometry; (b) roof-mounted arrays with the annual sun path for Ahmedabad (23.03° N). The panels are reproduced as supplied and are not to a common scale. Roof dimensions, surface areas and a north indicator were not recoverable from the archive and are listed in Section 5.5 among the required disclosures.

3.2 Modules and configurations

Three modules appear in the archive (Table 2). The Adani Elan Shine is a crystalline-silicon laminate rated 382 W_p; the UNI-SOLAR US-64 and US-128 are triple-junction amorphous-silicon laminates rated 64 W_p and 128 W_p. Both thin-film products are discontinued, and they are treated here as a low-efficiency archetype giving a controlled contrast against crystalline silicon at roughly 40% of its area-normalised performance, not as a procurement recommendation. The derived power density and standard-test-condition efficiency in the final rows differ by a factor of about 2.4 between the families and account for most of what follows.

Table 2. Module characteristics as recorded in the archive, with derived quantities. Power density and efficiency at standard test conditions (STC) are P_{max} divided by active area; the fill factor is P_{max} divided by the product of open-circuit voltage and short-circuit current.

Parameter	Adani Elan Shine	UNI-SOLAR US-64	UNI-SOLAR US-128
Cell technology (manufacturer)	**Crystalline silicon**	**Amorphous silicon (triple junction)**	**Amorphous silicon (triple junction)**
Cell type recorded in archive	**Crystalline silicon**	**Crystalline silicon**	**Crystalline silicon**
Cells in series (as recorded)	**144**	**36**	**66**
Active area, A (m^2)	**2.57**	**1.01**	**2.16**
Rated power, P_{max} (W_p)	**382**	**64**	**128**
Open-circuit voltage, V_{oc} (V)	**45.5**	**23.8**	**47.6**
Voltage at maximum power, V_{mp} (V)	**38.3**	**16.5**	**33.0**
Short-circuit current, I_{sc} (A)	**10.9**	**4.8**	**4.8**
Current at maximum power, I_{mp} (A)	**9.99**	**3.90**	**3.88**
Derived: $V_{mp} \times I_{mp}$ (W)	**382.6**	**64.3**	**128.0**
Derived: fill factor (–)	**0.770**	**0.560**	**0.560**
Derived: power density (W m^{-2})	**148.6**	**63.4**	**59.3**
Derived: efficiency at STC (%)	**14.86**	**6.34**	**5.93**

The archive crosses these three modules with four coverage treatments to give twelve configurations (Table 3): 50% of the exposed ground-floor terrace only; 50% of both roofs; 100% of the ground-floor terrace only; and 100% of both. Treatments are expressed in coverage blocks, one block being 50% of one floor's roof, giving one, two, two and four blocks. This is a proportional description rather than an area equivalence. Absolute areas in square metres, module counts and installed capacity in kilowatts-peak were not recorded, and Section 4.2 tests whether the two roofs behave as though equal in area rather than presuming it.

Table 3. Configurations and archived capital costs. GF = exposed ground-floor roof; FF = first-floor roof; one coverage block = 50% of one floor's roof.

Config.	Module	GF (%)	FF (%)	Blocks	Capital cost (₹)
C1	Adani Elan Shine (c-Si)	**50**	**0**	**1**	**310,625**
C2	Adani Elan Shine (c-Si)	**50**	**50**	**2**	**491,875**
C3	Adani Elan Shine (c-Si)	**100**	**0**	**2**	**491,875**
C4	Adani Elan Shine (c-Si)	**100**	**100**	**4**	**854,375**
C5	UNI-SOLAR US-64 (a-Si)	**50**	**0**	**1**	**298,125**
C6	UNI-SOLAR US-64 (a-Si)	**50**	**50**	**2**	**466,875**
C7	UNI-SOLAR US-64 (a-Si)	**100**	**0**	**2**	**466,875**
C8	UNI-SOLAR US-64 (a-Si)	**100**	**100**	**4**	**804,375**
C9	UNI-SOLAR US-128 (a-Si)	**50**	**0**	**1**	**298,125**
C10	UNI-SOLAR US-128 (a-Si)	**50**	**50**	**2**	**466,875**
C11	UNI-SOLAR US-128 (a-Si)	**100**	**0**	**2**	**466,875**
C12	UNI-SOLAR US-128 (a-Si)	**100**	**100**	**4**	**804,375**

3.3 Plausibility audit of the archived dataset

Because the archive cannot be re-run, its internal consistency and its agreement with independent reference points were tested directly. Four checks were applied. The first compares each module's rated power against the product of its maximum-power voltage and current, and computes the fill factor, which discriminates between crystalline and amorphous silicon independently of any declared label. The second converts each archived annual yield into an implied installed capacity using a regional specific yield, and thence into an implied module area using the power density of Table 2, so that configurations sharing one physical roof can be compared. The third compares the archived capital costs, expressed per unit of implied capacity, against the national benchmark. The fourth compares the archived demand against published metered consumption for Indian air-conditioned dwellings.

The specific yield used for the second check is 1450 to 1600 kWh kW_p^{-1} yr^{-1} for a fixed-tilt array in Gujarat, a range consistent with field performance reported for a grid-connected plant in a tropical semi-arid Indian environment (Malvoni et al., 2020). Implied capacity is E_g/Y_s and implied module area is that capacity divided by the module power density. Both are order-of-magnitude diagnostics rather than reconstructions of the original array, and they are used only to test whether the archived yields are mutually and physically consistent.

3.4 Settlement regime and energy matching

Settlement follows the Gujarat Electricity Regulatory Commission (Net Metering Rooftop Solar PV Grid Interactive Systems) Regulations, 2016, Notification No. 5/2016 of 18 June 2016, as subsequently amended (GERC, 2016). Regulation 2.1(p) defines net metering as an arrangement under which the rooftop system delivers surplus electricity to the distribution licensee after off-setting the electricity supplied to the consumer during the applicable billing period. For residential consumers, Regulation 9.2 provides that where supply exceeds generation the licensee invoices net consumption at the prevailing tariff, that where injection exceeds consumption in the billing period the excess is purchased at the average power purchase cost (APPC) rate determined by the Commission for the year of commissioning and fixed for the whole life of the system, and that banking is allowed within one billing cycle. The arrangement modelled here is therefore net metering with periodic set-off and surplus purchase, not a feed-in tariff and not net billing.

Two features of that regulation shape the analysis. Because banking is limited to one billing cycle, the set-off is determined by the billing-period energy balance rather than by instantaneous coincidence, so monthly rather than hourly resolution is the correct accounting basis for the financial settlement. Section 4.1 shows that archived generation exceeds demand in every month of every configuration, so the monthly set-off equals full monthly demand and the monthly and annual set-offs coincide exactly. Because the APPC is fixed in nominal terms at commissioning, real escalation is applied only to the set-off component, and the export component is held constant in real terms.

Since the applicable APPC determination for a given commissioning year was not available, and to test the sensitivity of the conclusions to regime design, results are reported between two bounds indexed by a settlement parameter κ:

$$\text{self-consumed} = \kappa \cdot \min(E_g, E_d), \quad \text{exported} = E_g - \text{self-consumed} \tag{1}$$

At κ = 1 the whole billing-period set-off is realised, which is the arrangement under Regulation 9.2 given that generation exceeds demand in every month. This is the upper-benefit bound. At κ = 0 no set-off is realised and the entire output is remunerated at the export rate, which corresponds to net billing or gross metering, the regimes compared by Aquila et al. (2024) and Pramadya and Kim (2024). This is the lower-benefit bound. Every financial indicator is reported as a range between the two. Self-sufficiency is not tabulated, because on a billing-period balance it equals unity for every configuration and carries no information. Instantaneous self-consumption, which would be considerably lower and matters for grid impact and storage sizing rather than for billing under net metering, cannot be evaluated without the hourly series.

3.5 Techno-economic model

Configurations are appraised over N = 25 years in constant 2024 Indian rupees. The gross annual benefit combines set-off at the retail tariff p_r with export at p_x, the former escalating in real terms at rate e and the latter fixed:

$$B_t = \kappa \cdot \min(E_{g,t}, E_d) \cdot p_r (1 + e)^{t-1} + [E_{g,t} - \kappa \cdot \min(E_{g,t}, E_d)] \cdot p_x \tag{2}$$

with generation declining at a constant rate δ so that $E_{g,t} = E_{g,1}(1 - \delta)^{t-1}$. Net cash flow subtracts annual operation and maintenance at a fraction ω of capital cost and one inverter replacement of fraction ρ in year t_{rep}:

$$CF_t = B_t - \omega \cdot C_0 - \rho \cdot C_0 \cdot [t = t_{rep}] \tag{3}$$

Net present value is $NPV = -C_0 + \Sigma\, CF_t(1 + r)^{-t}$, and the internal rate of return is the discount rate at which it vanishes. Simple and discounted payback are the times at which cumulative undiscounted and discounted cash flow first turn positive, the latter reported as undefined where the criterion is never met. The levelised cost of electricity is

$$LCOE = [\, C_0 + \Sigma_t\, (\omega \cdot C_0 + \rho \cdot C_0 \cdot [t = t_{rep}])\, (1 + r)^{-t}\,] \,/\, [\, \Sigma_t\, E_{g,t}\, (1 + r)^{-t}\,] \tag{4}$$

Avoided emissions are $E_g \cdot \varepsilon_g$, reported both for a constant emission factor and for one declining at 2% per year, since the Indian grid is decarbonising and a constant factor gives an upper bound.

3.6 Capital cost: archived structure and benchmark basis

The archived costs fit the form $C_0 = F + k \cdot n$, where n is the number of coverage blocks. The fitted fixed component F is ₹129,375 for all three families, covering inverter, protection, metering and connection, and the per-block component k is ₹181,250 for crystalline silicon and ₹168,750 for both thin-film modules, covering modules, mounting, cabling and labour. Cost therefore scales with area equipped rather than with rated capacity. The archived value for C4 was ₹804,375, identical to the two thin-film four-block values and inconsistent with its own family's cost line; the value implied by that line, ₹854,375, is used here and the discrepancy is noted. All costs are exclusive of goods and services tax and of any capital subsidy.

No quotations support these figures, so a second basis is constructed from published benchmarks. The Ministry of New and Renewable Energy benchmark effective 13 February 2024 is ₹50,000 per kW for the first 2 kW and ₹45,000 per kW thereafter (MNRE, 2024). Applying that schedule to the capacity implied by each archived yield gives a benchmark capital cost for every configuration. Results are reported on both bases throughout: the archived basis uses Table 3, and the benchmark basis uses per-kilowatt national rates. The two differ not only in level but in structure, since the archived basis makes cost proportional to area and the benchmark basis makes it proportional to capacity, and Section 4.5 shows that this structural difference changes which conclusions survive.

Table 4. Economic and environmental assumptions. Base values give the deterministic results of Section 4.4; ranges define the uniform marginals sampled in the sensitivity and Monte Carlo analyses.

Parameter	Base value	Range sampled	Basis
Analysis period, N	**25 yr**	**20–25 yr**	Conventional module performance-warranty term
Real discount rate, r	**8%**	**5–11%**	Household opportunity cost of capital in India
Retail tariff, p_r	**₹6.00 kWh⁻¹**	**₹5.00–7.50 kWh⁻¹**	Residential slab tariff recorded in the archive
Export tariff, p_x	**₹2.00 kWh⁻¹**	**₹1.50–3.00 kWh⁻¹**	APPC-based surplus purchase under GERC (2016) Reg. 9.2
Settlement regime, κ	**reported at 0 and 1**	**0–1**	κ = 1 net metering with set-off; κ = 0 net billing
Real escalation, e (set-off only)	**0% yr⁻¹**	**0–3% yr⁻¹**	APPC fixed in nominal terms for system life, so not escalated
Degradation, δ (c-Si / a-Si)	**0.7% / 1.0% yr⁻¹**	**0.5–1.2% yr⁻¹**	Jordan and Kurtz (2013); Choi et al. (2018); Malvoni et al. (2020)
O&M, ω	**1.0% of C_0 yr⁻¹**	**0.5–2.0%**	Cleaning, inspection and minor repair in a dusty climate
Inverter replacement, ρ	**10% of C_0, yr 12**	**fixed**	Single mid-life power-electronics replacement
Capital cost factor	**1.00**	**0.85–1.30**	Applied to whichever cost basis is in use
PV yield factor	**1.00**	**0.80–1.05**	Unmodelled soiling, mismatch, inverter and array-growth losses
Demand level factor	**1.00**	**1.0–5.0**	Archived demand is low against metered Indian dwellings
Specific yield, Y_s	**1,525 kWh kW_p^{-1}**	**1,450–1,600**	Fixed-tilt Gujarat; Malvoni et al. (2020)
Grid emission factor, ε_g	**0.716 t MWh⁻¹**	**constant or −2% yr⁻¹**	CEA CO_2 Baseline Database v19.0, FY 2022–23 (CEA, 2024)

3.7 Sensitivity, uncertainty and statistical treatment

Variance in net present value is apportioned among the eleven uncertain inputs of Table 4 by variance-based global sensitivity analysis, using the first-order estimator of Saltelli et al. (2010) and the Jansen total-order estimator, with N = 65,536 base samples and N(k + 2) = 851,968 model evaluations per configuration. First-order indices S_i measure the variance removed by fixing an input alone, total indices S_{Ti} include its interactions, and the difference quantifies interaction. This replaces squared correlation coefficients, which are valid only for additive monotone models and cannot detect interaction. Estimator sampling error is of order 0.01, so small negative differences are noise. A separate Monte Carlo of 40,000 realisations per configuration, sampling the same marginals independently, gives distributions of net present value and the probability of profitability under each cost basis. Inputs were treated as independent because no defensible dependence structure could be established, which is stated as an assumption. Calculations used Python 3.12 with NumPy, a PCG64 generator and fixed seed 20260811, so results reproduce exactly.

Energy quantities are held at their archived values throughout, and no energy data were resampled or synthesised. Two restrictions apply to the statistical treatment. Scaling of yield with coverage is reported as direct ratios rather than as a fitted regression, because four deterministic configurations spanning three distinct coverage levels cannot support inference about a physical scaling law. Correlation tests between the twelve monthly demand and generation shares are omitted, because with n = 12 serially dependent and strongly seasonal observations conventional significance testing would mislead; seasonal coincidence is reported instead as a distribution-free comparison of season blocks.

4. Results

4.1 Plausibility audit of the archived dataset

The audit is reported first, because it conditions how everything that follows should be read. Two checks pass and two fail.

The module parameters are internally consistent. For all three modules the product of maximum-power voltage and current reproduces the rated power to within 0.5% (382.6 against 382 W_p, 64.3 against 64, and 128.0 against 128). The fill factors, however, contradict the cell-type label carried in the archive. A fill factor of 0.770 for the Adani module is typical of crystalline silicon, whereas 0.560 for both UNI-SOLAR modules is characteristic of amorphous silicon, and the derived efficiencies of 6.34% and 5.93% are far below any crystalline product. The archive nonetheless records all three as crystalline, and assigns 36 and 66 cells in series to the two thin-film modules, implying per-cell voltages of 0.661 V and 0.721 V rather than the roughly 2.16 V of a triple-junction amorphous cell. The Adani entry of 144 cells implies 0.316 V per cell and is evidently a half-cell count. These are input-specification errors whose effect on the one-diode calculation cannot be quantified without re-running the model.

The archived yields are not mutually consistent with the stated geometry (Table 5). Converting each annual yield to an implied capacity at 1450 to 1600 kWh kW_p^{-1} yr^{-1} gives 4.7 to 66.7 kW_p across the twelve configurations, and dividing by module power density gives implied module areas of 75 to 828 m^2. Configurations C4, C8 and C12 all specify 100% of both roofs and therefore describe the same physical area, yet they imply 407 to 449 m^2, 300 to 331 m^2 and 750 to 828 m^2 respectively. These differ by a factor of up to 2.5, so at least two of the three cannot be reconciled with a single roof. The upper end of that range is also difficult to attribute to a two-storey detached dwelling with three cooled rooms. On capacity, implied values above roughly 20 kW_p sit well outside the residential envelope of India's subsidy programme, which is benchmarked on the first 2 kW and additional kilowatts (MNRE, 2024), although they remain within the 1 kW to 1 MW range that the net-metering regulation admits (GERC, 2016).

Table 5. Plausibility audit. Implied capacity is the archived annual yield divided by a specific yield of 1450 to 1600 kWh kW_p^{-1} yr^{-1}; implied module area is that capacity divided by the power density of Table 2. Archived cost per implied kilowatt is compared with the MNRE benchmark of ₹45,000 to ₹50,000 per kW (MNRE, 2024).

Config.	Module	GF/FF	E_g (kWh yr^{-1})	Implied capacity (kW_p)	Implied module area (m^2)	Archived cost (₹ per kW_p)
C1	c-Si	**50/0**	**31,593**	**19.7–21.8**	**133–147**	**14,300–15,700**
C2	c-Si	**50/50**	**60,679**	**37.9–41.8**	**255–282**	**11,800–13,000**
C3	c-Si	**100/0**	**56,360**	**35.2–38.9**	**237–262**	**12,700–14,000**
C4	c-Si	**100/100**	**96,707**	**60.4–66.7**	**407–449**	**12,800–14,100**
C5	a-Si US-64	**50/0**	**7,580**	**4.7–5.2**	**75–82**	**57,000–62,900**
C6	a-Si US-64	**50/50**	**15,194**	**9.5–10.5**	**150–165**	**44,600–49,200**
C7	a-Si US-64	**100/0**	**15,174**	**9.5–10.5**	**150–165**	**44,600–49,200**
C8	a-Si US-64	**100/100**	**30,400**	**19.0–21.0**	**300–331**	**38,400–42,300**
C9	a-Si US-128	**50/0**	**17,732**	**11.1–12.2**	**187–206**	**24,400–26,900**
C10	a-Si US-128	**50/50**	**35,556**	**22.2–24.5**	**375–414**	**19,000–21,000**
C11	a-Si US-128	**100/0**	**35,509**	**22.2–24.5**	**375–413**	**19,100–21,000**
C12	a-Si US-128	**100/100**	**71,157**	**44.5–49.1**	**750–828**	**16,400–18,100**

The cost audit shows that the archived costs are not uniformly low. Expressed per implied kilowatt they range from ₹12,400 to ₹15,000 for the crystalline configurations, ₹17,200 to ₹25,600 for the US-128 family and ₹40,400 to ₹60,000 for the US-64 family, against a benchmark of ₹45,000 to ₹50,000 per kW. The crystalline figures sit a factor of three to four below benchmark and the US-128 figures roughly a factor of two below, whereas the US-64 figures are broadly consistent with it. The apparent cost advantage in the archive is therefore specific to the crystalline family rather than general, which is why Section 4.5 reports every economic result on both cost bases.

The archived demand is also low. Annual totals of 916 to 980 kWh correspond to 2.5 to 2.7 kWh per day for a dwelling with three 1.5-ton units. A single unit drawing about 1.5 kW over the stated thirteen daily hours would consume roughly 590 kWh in a thirty-day month, whereas the archived whole-building total for May is 187 kWh. The archived demand is therefore about an order of magnitude below metered consumption for comparable Indian air-conditioned dwellings (Ramapragada et al., 2022). Since demand enters the economics only through the set-off, which the settlement bounds already span, this affects the interpretation of the matching results more than the financial ranges, and the Monte Carlo samples demand up to five times the archived level.

4.2 Demand, coverage and the shading effect

Archived demand tracks the cooling season closely, holding near 34 to 38 kWh per month from October to March and peaking in May. Only two distinct demand profiles appear across the twelve configurations, determined entirely by coverage: configurations sharing a coverage level differ by at most 1 kWh in any month. Module technology has no effect on demand, which is consistent with an array that modifies the roof heat balance by geometric obstruction rather than through any property of the cell material.

Table 6. Archived monthly and annual building electricity demand at the two coverage levels. Configurations sharing a coverage level differ by at most 1 kWh in any month.

Coverage	Jan	Feb	Mar	Apr	May	Jun	Jul	Aug	Sep	Oct	Nov	Dec	Annual
50% (C1, C2, C5, C6, C9, C10)	**36**	**34**	**36**	**131**	**187**	**161**	**100**	**77**	**108**	**38**	**37**	**35**	**980**
100% (C3, C4, C7, C8, C11, C12)	**36**	**34**	**36**	**117**	**171**	**149**	**92**	**73**	**98**	**38**	**37**	**35**	**916**
Reduction (kWh)	**0**	**0**	**0**	**14**	**16**	**12**	**8**	**4**	**10**	**0**	**0**	**0**	**64**
Reduction (%)	**0.0**	**0.0**	**0.0**	**10.7**	**8.6**	**7.5**	**8.0**	**5.2**	**9.3**	**0.0**	**0.0**	**0.0**	**6.5**

Doubling coverage lowers annual demand by 64 kWh, or 6.5%, entirely within the cooling season: 8.4% over April to September, 10.7% in April, and no change at all from October to March (Fig. 3). The pattern is consistent with a purely thermal mechanism, in which modules intercept short-wave radiation before it reaches the slab and the reduced gain has no electrical consequence where no cooling plant operates. Two qualifications apply. The result quantifies the increment from half to full coverage and not the benefit of installing photovoltaics at all, because the archive contains no zero-coverage reference case. The archive also records no thermal effect whatsoever from first-floor coverage, even though the first-floor roof caps a conditioned bedroom, which is discussed as an anomaly in Section 5.3.

Fig. 3. (a) Archived monthly demand at 50% and 100% roof coverage; the shaded band marks the April to September cooling season. (b) Demand reduction from doubling coverage, over the year, over the cooling season and in the month of largest effect.

4.3 Generation, scaling and cost-normalised yield

Archived annual generation spans more than an order of magnitude, from 7,580 kWh for the smallest thin-film configuration (C5) to 96,707 kWh for full crystalline coverage (C4). Within each thin-film family, yield scales with the area equipped: relative to the one-block case the ratios are 2.00, 2.00 and 4.01 for the US-64 family and 2.01, 2.00 and 4.01 for the US-128 family, against 2.00, 2.00 and 4.00 under exact proportionality. Two observations follow. The near-identity of the two two-block treatments, 50% of both roofs against 100% of the ground-floor roof, is consistent with the two roof areas being similar, although it does not establish this independently. Proportionality this precise also indicates that no penalty was applied as the array grew, so no inter-row shading, incremental mismatch or edge effect is represented. The crystalline family does not follow the pattern, returning 1.92, 1.78 and 3.06, which is inconsistent with both thin-film families and with a fixed geometry. That departure is treated in Section 5.5 as an unresolved feature of the archive rather than as a physical result.

Module technology produces the larger effect, and one predictable from Table 2. At one coverage block the crystalline configuration generates 31,593 kWh against 7,580 kWh for the US-64 and 17,732 kWh for the US-128, factors of 4.2 and 1.8, at an archived capital cost only 4% higher. Recast against capital cost (Fig. 4a), the three technologies occupy separated trajectories that never cross, so no amount of additional thin-film coverage reaches the crystalline yield at equal archived expenditure. Normalising by cost (Fig. 4b) gives 102 to 123 kWh yr^{-1} per ₹1,000 for the crystalline configurations, 60 to 89 for the US-128 and 25 to 38 for the US-64. Within each family the multi-block treatments outperform the single-block treatment because the fixed ₹129,375 is spread further, but the gain saturates quickly. Section 4.5 shows that this ordering by cost-normalised yield is specific to the archived, area-proportional cost structure.

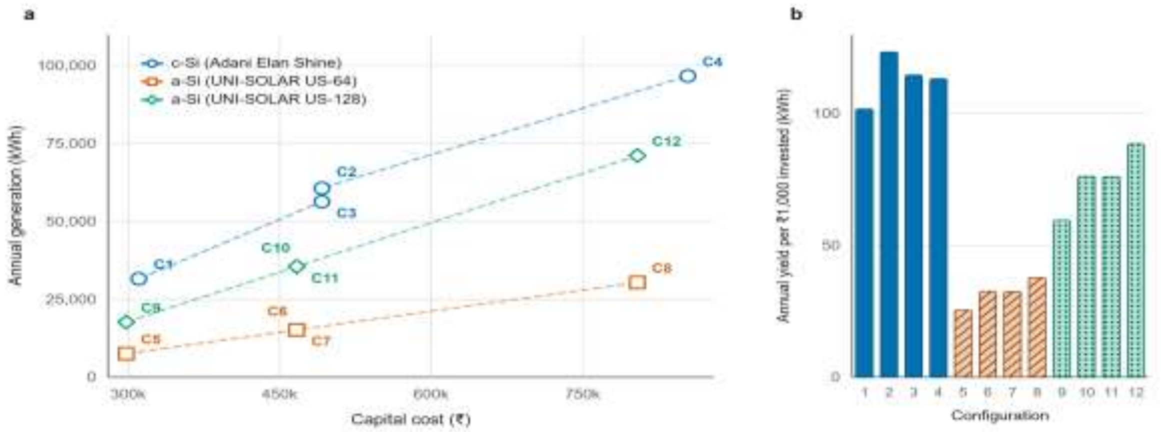

Fig. 4. (a) Archived annual generation against archived capital cost; dashed lines connect the four coverage treatments within each module family. (b) Annual generation per ₹1,000 of archived capital cost.

4.4 Seasonal coincidence between generation and demand

Generation and demand are not complementary. Normalised profiles (Fig. 5a) show generation peaking in March under clear pre-monsoon skies and reaching its minimum in July and August under monsoon cloud, while demand peaks in May and stays elevated through the monsoon because heat and humidity sustain the cooling load after insolation collapses. Expressed as season blocks, which requires no distributional assumption (Fig. 5b), June to September carries 45.5% of annual demand but only 27.2% of crystalline generation and 23.1% of US-128 generation. March to May carries 36.1% of demand against 28.4 to 30.5% of generation, and October to February carries just 18.4% of demand against 44.1 to 46.4% of generation. Nearly half of annual output therefore falls in the third of the year when the building needs least.

The demand profile is far more variable than any generation profile, with a coefficient of variation across months of 64.6% against 14.8 to 24.3%, and a ratio of highest to lowest month of 5.50 against 1.67 to 2.46. Among the modules, crystalline silicon gives the flattest annual profile and the US-128 the most monsoon-sensitive, with best-to-worst month ratios of 1.67 and 2.46. Since the two thin-film laminates are nominally the same technology, that divergence is larger than physical reasoning supports and is listed in Section 5.5 alongside the cell-parameter errors identified in Section 4.1, which are its most likely cause.

Fig. 5. (a) Monthly demand and generation, each normalised to its own annual total so that profiles of very different magnitude are comparable; the shaded band marks the monsoon. (b) The same information aggregated into pre-monsoon, monsoon and mild-season blocks.

4.5 Techno-economic performance under both settlement regimes

Archived generation exceeds demand by factors of 8 to 105, so the billing-period set-off is capped at 0.95 to 12.9% of output and export supplies 87 to 100% of benefit depending on the regime. Generation also exceeds demand in every month of every configuration, the smallest ratio being 3.27 for C5 in June, so the monthly set-off equals full monthly demand and the κ = 1 bound is the exact settlement under Regulation 9.2 rather than an optimistic approximation. Every configuration in the archive behaves economically as a small merchant generator rather than as a bill-reduction measure.

Config.	Module	Set-off cap (%)	kWh per ₹1,000	SPB (yr)	DPB (yr)	NPV (₹)	IRR (%)	LCOE (₹ kWh^{-1})
C1	c-Si	**3.10**	**101.7**	**4.92–5.25**	**6.54–7.13**	**281,188–323,033**	**18.1–19.5**	**1.12**
C2	c-Si	**1.62**	**123.4**	**4.13–4.28**	**5.24–5.47**	**660,127–701,972**	**22.6–23.5**	**0.92**
C3	c-Si	**1.63**	**114.6**	**4.47–4.62**	**5.78–6.03**	**573,002–612,115**	**20.8–21.6**	**0.99**
C4	c-Si	**0.95**	**113.2**	**4.59–4.69**	**5.97–6.13**	**971,307–1,010,419**	**20.5–21.0**	**1.00**
C5	a-Si US-64	**12.94**	**25.4**	**22.49–n/a**	**n/a**	**−192,475 to −150,587**	**−1.9–0.8**	**4.58**
C6	a-Si US-64	**6.45**	**32.5**	**18.98–22.68**	**n/a**	**−235,957 to −194,112**	**0.8–2.3**	**3.58**
C7	a-Si US-64	**6.04**	**32.5**	**19.21–22.73**	**n/a**	**−236,351 to −197,239**	**0.7–2.2**	**3.58**
C8	a-Si US-64	**3.01**	**37.8**	**17.09–18.55**	**n/a**	**−323,354 to −284,242**	**2.5–3.2**	**3.08**
C9	a-Si US-128	**5.53**	**59.5**	**8.49–9.62**	**16.66–23.02**	**7,502–49,348**	**8.3–10.0**	**1.96**
C10	a-Si US-128	**2.76**	**76.2**	**6.83–7.27**	**10.47–12.40**	**165,140–206,985**	**12.2–13.2**	**1.53**
C11	a-Si US-128	**2.58**	**76.1**	**6.87–7.28**	**10.56–12.43**	**164,214–203,327**	**12.2–13.1**	**1.53**
C12	a-Si US-128	**1.29**	**88.5**	**5.98–6.16**	**8.58–8.93**	**479,490–518,602**	**14.9–15.5**	**1.32**

Table 7 reports each indicator as a range between the two settlement bounds on the archived cost basis. The ranges are narrow, because export dominates under either regime: moving from net metering to net billing lengthens simple payback by 0.10 to 1.13 years and reduces net present value by 4 to 28%, with the largest effects on the smallest systems, which have the highest set-off share. On this basis the crystalline configurations recover capital in 4.13 to 5.25 years undiscounted and 5.24 to 7.13 years discounted, with internal rates of return of 18.1 to 23.5% and levelised costs of ₹0.92 to 1.12 kWh^{-1}. The US-128 configurations are weaker, with discounted paybacks of 8.58 to 23.02 years and levelised costs of ₹1.32 to 1.96 kWh^{-1}. The four US-64 configurations return levelised costs of ₹3.08 to 4.58 kWh^{-1}, negative net present values throughout, and discounted cash flow that never turns positive within 25 years. That failure is invisible to simple payback, which returns finite values of 17.1 to 22.7 years for the same configurations.

Table 7. Techno-economic indicators on the archived cost basis, reported as ranges between the two settlement bounds (net billing, $\kappa = 0$, to net metering, $\kappa = 1$). LCOE and cost-normalised yield do not depend on the settlement regime. n/a indicates that discounted cash flow never turns positive within the analysis period.

The two leading configurations differ according to the criterion applied. C2, at half coverage of both roofs, minimises payback, maximises internal rate of return, achieves the lowest levelised cost and the highest cost-normalised yield. C4, at full coverage, maximises net present value and avoided emissions. This is the standard divergence between rate-based and scale-based criteria rather than a contradiction. Marginal analysis sharpens the point: each added coverage block costs ₹6.23 to 10.06 per additional annual kWh for crystalline silicon, ₹9.47 to 9.49 for the US-128 and ₹22.16 to 22.22 for the US-64. Using the capital cost as originally tabulated rather than the corrected value, the C2 to C4 step would be ₹8.67 rather than ₹10.06.

Rebasing capital cost to national per-kilowatt benchmarks changes the picture qualitatively, not merely in level (Fig. 6b). Levelised costs converge to ₹3.37 to 3.59 kWh^{-1} across all twelve configurations, a spread of 6% where the archived basis gave a spread of a factor of five. The reason is structural: when cost scales with capacity and capacity scales with generation, unit cost becomes almost independent of technology, and the advantage of high efficiency no longer shows up in the cost per kilowatt-hour. On the benchmark basis no configuration returns a positive net present value at an export tariff of ₹2.00 kWh^{-1} under either settlement regime, and the break-even export tariff rises to ₹3.19 to 3.59 kWh^{-1} for every configuration. Break-even capital-cost multipliers on the archived basis make the same point from the other direction: 1.79 to 2.24 for the crystalline configurations, 1.02 to 1.56 for the US-128 and 0.44 to 0.69 for the US-64, so the crystalline advantage disappears once archived costs rise by rather more than a factor of two.

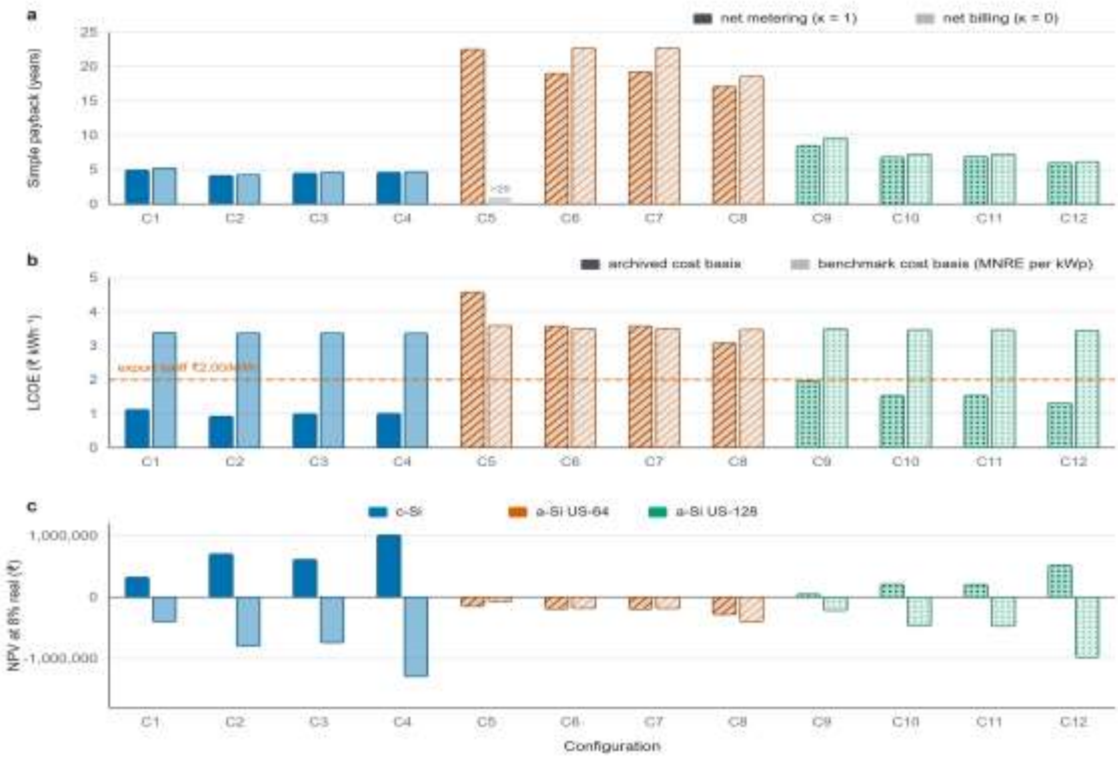

Fig. 6. Economic performance across settlement regimes and cost bases: (a) simple payback under net metering and net billing, with grey stubs marking configurations exceeding 25 years; (b) levelised cost on

the archived and benchmark cost bases against the export tariff; (c) net present value under net metering on both cost bases. Fills distinguish the module families by colour and texture.

4.6 Sensitivity and uncertainty

Variance-based sensitivity analysis for C2 on the archived cost basis (Fig. 7a) gives the export tariff a first-order index of 0.532 and a total index of 0.542, followed by the discount rate (0.257, 0.273), the photovoltaic yield factor (0.095, 0.096) and the capital-cost factor (0.056, 0.056). The settlement regime κ contributes only 0.017, which quantifies why the bounds in Table 7 are narrow, and the demand level, lifetime, operating cost, degradation rate, retail tariff and escalation together account for under 0.03. First-order indices sum to 0.980, so interactions account for 2% of variance and the model is close to additive over these ranges. The finding that the retail tariff is almost irrelevant while the export tariff dominates follows directly from the 87 to 100% export share and inverts the usual emphasis in residential rooftop appraisal.
The break-even export tariff (Fig. 7b) expresses the same exposure in interpretable units. On the archived cost basis the crystalline configurations remain viable down to ₹0.83 to 1.12 kWh^{-1} across both regimes, the US-128 configurations break even at ₹1.25 to 1.96 kWh^{-1}, and the US-64 configurations require ₹2.98 to 4.58 kWh^{-1}, above any plausible surplus-purchase rate. On the benchmark cost basis all twelve require ₹3.19 to 3.59 kWh^{-1}.

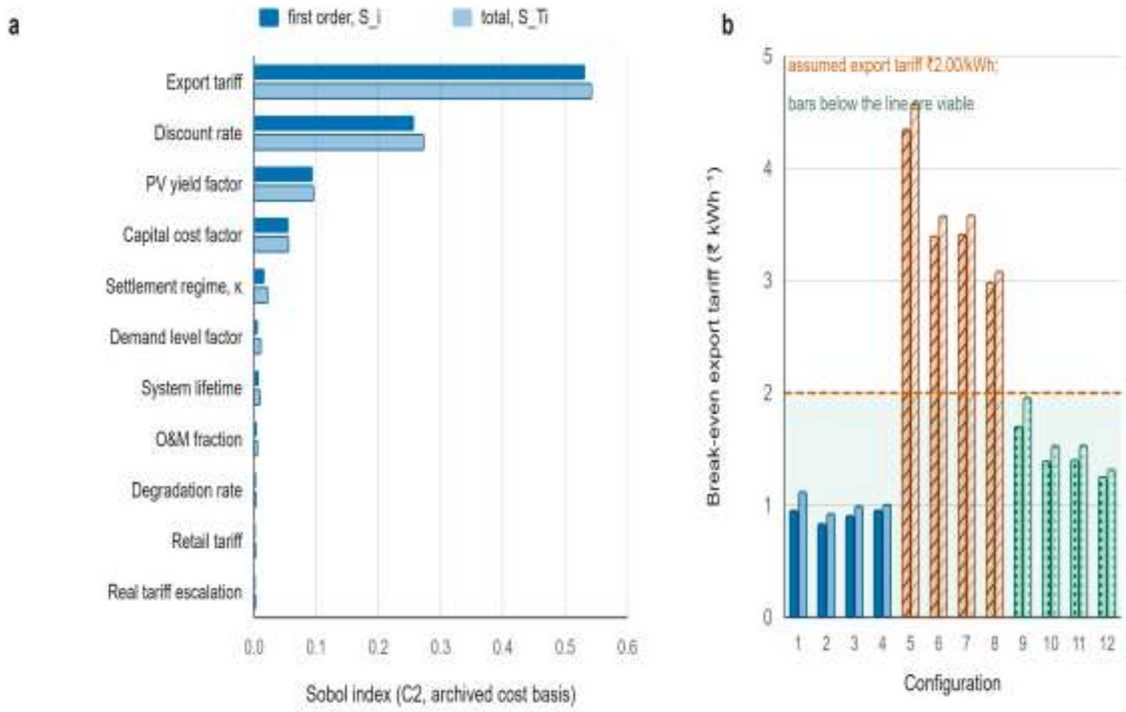

Fig. 7. (a) First-order and total Sobol indices for the net present value of C2 on the archived cost basis (N = 65,536; sampling error of order 0.01). (b) Export tariff at which each configuration reaches zero net present value, under net metering and net billing.

The Monte Carlo results (Table 8, Fig. 8) combine all eleven uncertainties. On the archived cost basis the crystalline configurations return positive net present value in 98.5 to 99.8% of 40,000 realisations and the US-128 configurations in 67.2 to 91.5%, while the US-64 configurations are profitable in only 3.9 to 5.7%. On the benchmark cost basis every family collapses: the probability of profitability falls to 0.8 to 1.7% for crystalline silicon, 0.9 to 4.1% for the US-128 and 1.7 to 18.2% for the US-64, the last being the family whose archived costs were already close to benchmark and which therefore changes least. No configuration is more likely than not to be profitable on the benchmark basis.

Table 8. Monte Carlo results (40,000 realisations per configuration; marginals from Table 4, including the settlement regime κ sampled over [0, 1]) under the two capital-cost bases.

Config.	Module	P(NPV>0) archived	NPV P50 archived (₹)	NPV P90 archived (₹)	P(NPV>0) benchmark	NPV P50 benchmark (₹)	Break-even CAPEX multiplier
C1	c-Si	98.5%	305,639	554,234	1.7%	−480,417	1.79–1.91
C2	c-Si	99.8%	653,805	1,105,989	1.1%	−975,598	2.17–2.24
C3	c-Si	99.4%	564,804	989,845	1.0%	−905,354	2.02–2.09
C4	c-Si	99.1%	896,769	1,617,922	0.8%	−1,593,241	1.99–2.03
C5	a-Si US-64	4.8%	−154,236	−39,249	18.2%	−75,324	0.44–0.56
C6	a-Si US-64	4.6%	−210,747	−53,210	5.3%	−200,607	0.56–0.64
C7	a-Si US-64	3.9%	−215,966	−60,666	4.6%	−205,173	0.56–0.63
C8	a-Si US-64	5.7%	−337,877	−65,194	1.7%	−464,932	0.65–0.69
C9	a-Si US-128	67.2%	49,251	207,787	4.1%	−244,879	1.02–1.14
C10	a-Si US-128	84.4%	187,375	470,063	1.5%	−546,914	1.31–1.39
C11	a-Si US-128	83.9%	187,765	464,132	1.4%	−551,152	1.31–1.38
C12	a-Si US-128	91.5%	467,151	1,004,765	0.9%	−1,161,669	1.52–1.56

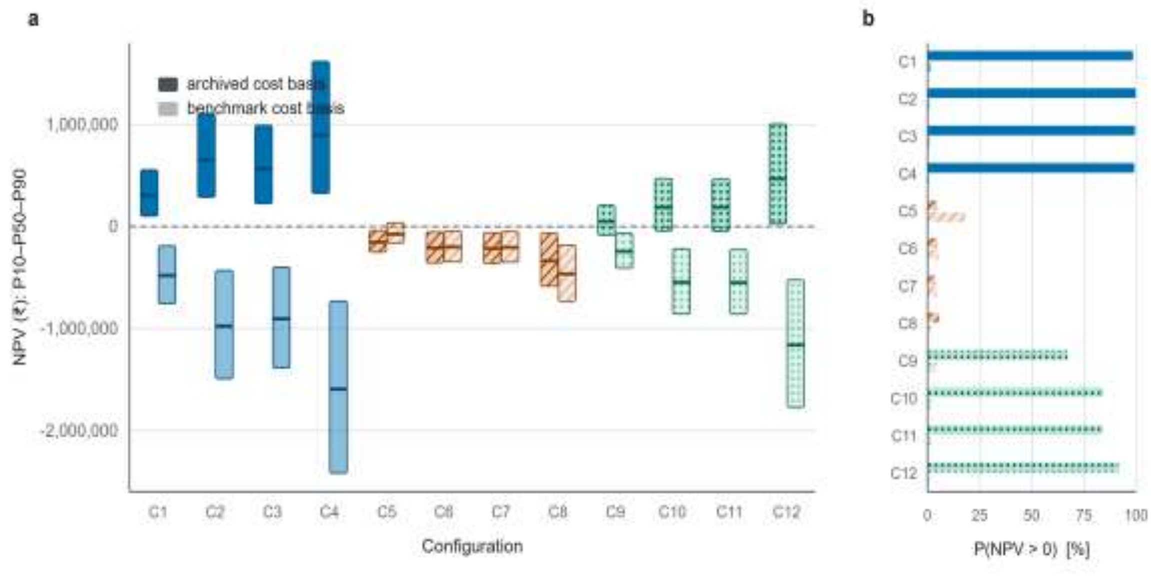

Fig. 8. (a) Monte Carlo distributions of net present value on the archived (solid) and benchmark (pale) cost bases; boxes span the tenth to ninetieth percentiles and the rule marks the median. (b) Probability of a positive net present value on each basis.

4.7 Carbon mitigation

Applying the current average emission factor of the Indian grid, 0.716 t CO_2 MWh^{-1} (CEA, 2024), avoided emissions range from 5.4 t yr^{-1} for C5 to 69.2 t yr^{-1} for C4. Cumulated over 25 years with degradation and a constant factor, this gives 520 to 1,593 t for the crystalline configurations, 282 to 1,132 t for the US-128 and 121 to 484 t for the US-64. These are upper bounds in three respects: an average factor represents the current fleet rather than the plant displaced at the margin, no allowance is made for curtailment of exported energy, and the factor will fall as the grid decarbonises. Imposing an illustrative decline of 2% per year reduces every 25-year total by 20%, to 416 to 1,273 t for the crystalline configurations. Because the factor is applied uniformly, these results rank configurations identically to annual yield and are reported for completeness rather than as an independent discriminator. No life-cycle assessment of the modules was performed, so no claim is made here about embodied impacts, which would bear particularly on the thin-film options given their larger area per unit of energy delivered.

5. Discussion

5.1 How capital cost is attributed decides whether technology matters

The factorial design separates two levers that are often treated as interchangeable, and in the archive they behave differently. Coverage multiplies output in proportion to the area equipped, so quadrupling it quadruples generation and the variable part of capital cost together and leaves their ratio essentially unchanged. Its only economic effect comes through dilution of the fixed ₹129,375, which is why cost-normalised yield improves from 102 to 123 kWh per ₹1,000 between C1 and C2 and then barely moves. Coverage is a decision about how much to invest rather than about how well.

Module technology appears to act on quality, but only under one costing convention. On the archived basis, where cost scales with area, the crystalline configuration generates 4.2 times the US-64 output for 4% more capital, so efficiency translates directly into lower unit cost and every US-64 increment destroys value. Rebasing to per-kilowatt benchmarks removes that translation entirely: levelised costs converge to within 6% across all twelve configurations, because cost then follows capacity and capacity follows generation. This is not a minor calibration difference. It means the frequently repeated claim that high-efficiency modules are economically superior on residential rooftops holds only where balance-of-system cost is genuinely area-driven, which is the case for mounting, cabling and labour but not for modules and inverters. Where per-watt costing applies, efficiency does not reduce unit cost; it reduces the area needed for a given capacity, and its value therefore depends on whether roof area binds. Both routes lead to the same practical advice on a constrained roof, but for different reasons and with different implications for a roof that is not constrained.

The precision of the proportional scaling carries a modelling caution. Ratios of 2.00 and 4.01 indicate that no penalty was applied as the array grew, whereas real arrays incur inter-row and self-shading, mismatch, longer direct-current runs and inverter clipping at higher packing densities. Ren et al. (2023) show that representing these changes optimal packing decisions materially. Archived generation for the larger configurations should therefore be read as an upper bound, and the advantage of full over half coverage is, if anything, overstated. The yield factor of 0.80 to 1.05 in Table 4 is intended to carry this bias, and the sensitivity analysis attributes about 10% of variance in net present value to it.

5.2 An export-dominated regime, and what it implies for policy

The most consequential result is not about hardware. Archived generation exceeds demand by factors of 8 to 105, so the billing-period set-off is capped at 12.9% of output and 87 to 100% of benefit is exposed to the export tariff. The Sobol analysis makes the consequence quantitative: the export tariff accounts for 53% of first-order variance in net present value against under 1% for the retail tariff, and the settlement regime itself accounts for under 2%. A household in this position is not meaningfully reducing its bill; it is selling power to the licensee using its roof, and it does so at a rate fixed at commissioning for the life of the system under Regulation 9.2.

This places the archived case at an extreme of the distribution reviewed by Luthander et al. (2015), who report residential self-consumption near 30% without storage. The difference is one of sizing rather than climate, since the arrays were dimensioned to the roof rather than to the load. Nor can the condition be escaped by modest demand growth: holding generation fixed, the set-off cap for C2 rises only from 1.6% to 8.1% at five times the archived demand and to 16.2% at ten times, and the Monte Carlo, which samples demand up to five times the archived level, attributes under 1% of variance to it. Since the archived demand is itself low against metered Indian air-conditioned dwellings (Ramapragada et al., 2022), the export exposure is structural rather than an artefact of one demand assumption.

The policy reading follows and diverges from prevailing emphasis. India's principal residential instrument, the PM Surya Ghar Muft Bijli Yojana, works chiefly through capital subsidy (MNRE, 2024), yet the capital-cost factor accounts for about 6% of variance in project value here while the export tariff accounts for 53%. For export-dominated systems, certainty in the surplus-purchase rate acts on 25 years of revenue whereas a capital grant acts once, and the regulatory design that fixes the APPC at commissioning transfers long-run price risk to the prosumer in a way a one-off grant does not offset. The break-even values quantify the exposure on the archived cost basis: crystalline configurations tolerate a fall to ₹0.83 to 1.12 kWh^{-1}, while the US-128 configurations break even at ₹1.25 to 1.96 kWh^{-1} and would be marginal under a revision of the magnitude Indian regulators periodically enact. This reinforces from the household side what Aquila et al. (2024) showed for net metering against net billing, what Pramadya and Kim (2024) found comparing settlement rules with installation incentives, and what Saez et al. (2024) quantified for Spanish surplus compensation. Alhammami and An (2021) report the same primacy of tariff design in a comparably sunny setting. One caveat is important: the ₹2.00 kWh^{-1} used here is a stated assumption varied over ₹1.50 to 3.00, not the APPC determination for any particular commissioning year, and the applicable determination should be substituted before the policy inference is relied upon quantitatively.

5.3 Seasonal mismatch and the shading co-benefit

In Ahmedabad the solar resource peaks before the monsoon while cooling demand persists through it, so the four months carrying 45.5% of demand receive 23 to 27% of generation, and the mild third of the year with 18.4% of demand receives 44 to 46% of output. This distinguishes hot semi-arid Indian conditions from the temperate settings in which much of the photovoltaic-shading literature developed. In Mediterranean and continental climates summer irradiance and cooling demand rise together and the heating season carries the penalty (Kapsalis et al., 2014; Kapsalis and Karamanis, 2015), whereas here there is no heating season but the monsoon severs the alignment exactly when cooling is needed. Under net metering with monthly banking the mismatch has limited financial consequence, because the set-off is already saturated in every month. It matters instead for grid impact, for the value of storage, and for any regime that settles at finer temporal resolution. Among the modules, the flatter crystalline profile, with a best-to-worst month ratio of 1.67 against 2.46 for the US-128, would be worth more under any such regime.

The shading co-benefit is real but small. Doubling coverage reduces archived annual demand by 6.5%, concentrated wholly in April to September and reaching 10.7% in April, through the interception mechanism established by measurement (Dominguez et al., 2011; Odeh and Pearling, 2025) and by simulation across climates (Wang et al., 2020; Ma et al., 2023). The magnitude is smaller than several published figures for reasons that are explicable rather than contradictory. Dominguez et al. (2011) reported a 38% cooling-load reduction against a bare roof, whereas the present figure is an increment between half and full coverage with roughly half the benefit already in the baseline. The roof also carries expanded-polystyrene insulation, which reduces the conductive pathway shading acts upon, and only three zones are cooled, so shading elsewhere yields comfort improvements that never appear as electricity. Bhuvad and Udayraj (2022) likewise found the benefit largest in hot and dry Indian zones and strongly dependent on roof construction. In monetary terms the co-benefit is minor: 64 kWh yr^{-1} avoided is worth ₹384 at the retail tariff, against annual generation benefits 50 to 500 times larger. It should be presented as a co-benefit rather than as a justification.

One archived result does not conform to this mechanism. Adding modules to the first-floor roof changes demand not at all, while ground-floor coverage produces the entire effect, even though the first-floor roof caps a conditioned bedroom where a shading benefit would be expected. The most likely explanation is that the first-floor array was represented in a way that did not participate in the surface heat balance. Since the model cannot be inspected, this is recorded as an unresolved feature of the archive rather than as a physical finding, and the shading results should be read with that in mind.

5.4 What is robust, what is not, and what follows for appraisal

Three conclusions of this analysis have different standing, and the distinction matters more than any of them individually.

The export dependence is robust. It follows arithmetically from generation exceeding demand by an order of magnitude or more, it survives every cost basis and both settlement regimes, and it would strengthen under any regime that settles at finer temporal resolution. It does not depend on the archived costs being correct.

The ordering of configurations is conditional on the cost structure rather than on the cost level. A uniform rescaling of the archived costs preserves the levelised-cost ordering exactly, because levelised cost is proportional to capital cost for fixed discount rate, operating cost, degradation and yield. Replacing area-proportional costing with per-kilowatt costing does not preserve it, and instead collapses the ordering almost entirely. The technology conclusion therefore holds within the archived costing convention and not beyond it.

Absolute viability is not established at all. On the archived basis the crystalline configurations look strongly attractive; on a benchmark basis consistent with current Indian prices no configuration returns positive value at ₹2.00 kWh^{-1} under either settlement regime, and every probability of profitability falls below 20%. Since the archived crystalline costs sit a factor of three to four below benchmark per implied kilowatt, the benchmark basis is the more likely description of a real installation. This analysis therefore establishes a ranking under a stated costing convention rather than a business case, and any statement of the form "payback is four years" is conditional on a cost basis that dated quotations would be needed to substantiate.

The four US-64 configurations also make a methodological point cleanly. Their simple paybacks of 17.1 to 22.7 years read as merely unattractive, yet their discounted cash flow never turns positive, their net present values are negative throughout, and their internal rates of return of −1.9 to 3.2% fall below any defensible cost of capital. A screening rule of the form "accept if payback is under twenty years" would admit three of the four under net metering. Payback is not uninformative, since across these twelve configurations it ranks identically to internal rate of return and levelised cost, but it cannot establish whether a project should be built, because it ignores the discount rate. Reporting net present value, internal rate of return and levelised cost alongside it, and comparing levelised cost against the tariff at which output is actually settled rather than against the retail tariff, separates the ranking question from the accept-or-reject question.

For practitioners in comparable settings, four implications follow. Establish first whether balance-of-system cost is area-driven or capacity-driven, because that determines whether module efficiency buys lower unit cost or only lower area. Size the array against the settlement regime rather than the roof, since an array many times the load converts a bill-offset proposition into a merchant one at a much lower unit price. Evaluate each option against its break-even export tariff, which states in one number how much regulatory tightening it can absorb. Expect the shading co-benefit without underwriting the investment with it.

5.5 Limitations and required disclosures

The central limitation is one of provenance. This is a re-analysis of an archived dataset whose model files, hourly outputs and array specifications are unavailable, so the simulations cannot be re-run, several archived features cannot be checked at source, and no independent party can reproduce the energy results from the inputs. That is a material reproducibility constraint, and it bounds every conclusion above. The following list states what a future study with access to the model would need to supply.

Array specification. Installed direct-current capacity, module count, actual covered area, series and parallel arrangement, tilt, azimuth, row spacing, inverter rating and efficiency, clipping and system losses. Without these, specific yield in kWh kW_p^{-1} yr^{-1}, performance ratio as defined by IEC 61724-1 (IEC, 2021) and capacity factor cannot be reported, yield is normalised by capital cost instead, and the results cannot be benchmarked against field studies such as Malvoni et al. (2020). Section 4.1 shows why this matters: the implied areas for the three configurations that share one roof differ by a factor of up to 2.5.

Hourly series. Instantaneous self-consumption, grid-impact metrics and the value of storage all require sub-daily data. Under net metering with monthly banking the billing-period balance governs the financial settlement, so the ranges in Table 7 are not widened by this gap, but any move to finer-resolution settlement or any storage assessment would require it.

Model inputs requiring confirmation. The cooling schedule spans thirteen hours although described as nine; the archived demand implies September cooling although the schedule states April to August; conditioned floor area, occupancy, infiltration and equipment coefficient of performance are unrecorded; the cell type recorded for both UNI-SOLAR modules contradicts their fill factors and derived efficiencies; the series-cell counts imply per-cell voltages inconsistent with the declared technologies; the crystalline family departs from the proportional scaling followed by both thin-film families; and first-floor coverage produces no thermal effect. Until these are resolved the crystalline scaling behaviour, the thin-film seasonal profiles and the shading results should be treated as provisional.

Validation and generality. No comparison against metered consumption was possible, so no NMBE or CV(RMSE) is reported and the demand series is unvalidated; the discrepancy between as-designed and as-built performance is well documented (Eon et al., 2020). The archive describes one dwelling under one typical-year weather file in one climate zone, with fixed occupancy and appliance schedules, whereas outcomes are known to be sensitive to occupant-driven uncertainty (Kotireddy et al., 2019; Chaturvedi et al., 2020) and to future weather (Liu et al., 2020). No zero-coverage control exists, so the absolute shading benefit is unquantified. Generalisation requires new simulation rather than extrapolation.

Cost and tariff evidence. The archived costs are not supported by quotations, and their implied cost per kilowatt varies from a factor of three to four below the national benchmark for the crystalline family to broadly consistent with it for the US-64 family. Dated per-watt quotations with a documented breakdown would allow the two-basis presentation to be replaced by a single substantiated basis. The export tariff is a stated assumption rather than the APPC determination for a specific commissioning year, and the applicable determination should be substituted.

Further modelling simplifications. Soiling enters only implicitly through the operating allowance rather than as an explicit optical loss, which matters in a dusty semi-arid environment; the decomposition of hourly insolation into direct and diffuse components is a recognised error source (An et al., 2020); no battery storage or demand shifting was considered; the Monte Carlo treats inputs as independent because no defensible dependence structure could be established; and carbon results use an average rather than a marginal emission factor with no life-cycle assessment of the modules (Sherwani et al., 2010).

6. Conclusions

This paper re-analysed an archived set of EnergyPlus results for a two-storey dwelling in Ahmedabad, covering a full factorial of three module technologies against four roof-coverage levels, and appraised all twelve configurations on discounted measures under two settlement regimes and two capital-cost bases with variance-based sensitivity analysis. Four conclusions follow, stated at the strength the evidence supports.

First, the economics of this class of system are governed by the export tariff. Archived generation exceeded demand by 8 to 105 times, capping the billing-period set-off at 0.95 to 12.9% of output and exposing 87 to 100% of benefit to export. The export tariff accounted for 53% of first-order variance in net present value against under 1% for the retail tariff and under 2% for the settlement regime. The break-even export tariff, ₹0.83 to 1.12 kWh^{-1} for crystalline configurations against ₹2.98 to 4.58 kWh^{-1} for the US-64 family on the archived cost basis, is proposed as a compact measure of exposure to regulatory change. This conclusion is arithmetic in origin and does not depend on the archived costs being correct.

Second, coverage and technology are not interchangeable, but the apparent superiority of high-efficiency modules is contingent on how capital cost is attributed. Generation scaled in proportion to the area equipped, with ratios of 2.00 and 4.01 against one coverage block for both thin-film families, so coverage set the size of the investment while leaving its quality nearly unchanged. Under the archived area-proportional cost structure the crystalline configurations achieved levelised costs of ₹0.92 to 1.12 kWh^{-1} against ₹3.08 to 4.58 kWh^{-1} for the US-64 family. Under per-kilowatt benchmark costing the twelve configurations converged to ₹3.37 to 3.59 kWh^{-1} and the technology distinction in unit cost disappeared, leaving roof area rather than cost as the binding constraint.

Third, absolute viability is not established. On the benchmark cost basis no configuration returned a positive net present value at ₹2.00 kWh^{-1} under either settlement regime, and no probability of profitability exceeded 20%. Since the archived crystalline costs sit a factor of three to four below the national benchmark per implied kilowatt, this analysis should be read as establishing a ranking under a stated costing convention rather than a business case. Payback screening compounds the difficulty, assigning finite values of 17.1 to 22.7 years to four configurations that a discounted appraisal rejects outright.

Fourth, generation and cooling demand are not seasonally complementary in this climate. June to September carried 45.5% of demand but 23 to 27% of generation, while the mild months with 18.4% of demand received 44 to 46% of output. Under net metering with monthly banking this has limited financial consequence, but it matters for grid impact, for storage value and for any finer-resolution settlement regime. The associated shading co-benefit was real but modest, doubling coverage reducing annual demand by 6.5%, worth roughly ₹384 per year against generation benefits 50 to 500 times larger.

The plausibility audit also constrains what the archive can support. The module fill factors contradict the recorded cell types, the implied module areas for three configurations sharing one roof differ by a factor of up to 2.5, and the archived demand is about an order of magnitude below metered Indian air-conditioned dwellings. Priorities for further work follow directly: recover or rebuild the model and archive its array specification so that specific yield and performance ratio can be reported and benchmarked; validate the demand model against metered consumption; add a zero-coverage control; substitute dated per-watt quotations and the applicable APPC determination; and repeat the factorial design across the Indian climate zones to establish where the export-dominated regime described here begins and ends.

References

1. Alhammami, H., An, H., 2021. Techno-economic analysis and policy implications for promoting residential rooftop solar photovoltaics in Abu Dhabi, UAE. Renewable Energy 167, 359–368. https://doi.org/10.1016/j.renene.2020.11.091
2. An, J., Yan, D., Guo, S., Gao, Y., Peng, J., Hong, T., 2020. An improved method for direct incident solar radiation calculation from hourly solar insolation data in building energy simulation. Energy and Buildings 227, 110425. https://doi.org/10.1016/j.enbuild.2020.110425
3. Aquila, G., Rotella Junior, P., Rocha, L.C.S., Balestrassi, P.P., Pamplona, E.O., Nakamura, W.T., 2024. Net metering rolling credits vs. net billing buyback: An economic analysis of a policy option proposal for photovoltaic prosumers. Renewable Energy 232, 121154. https://doi.org/10.1016/j.renene.2024.121154
4. Behura, A.K., Kumar, A., Rajak, D.K., Pruncu, C.I., Lamberti, L., 2021. Towards better performances for a novel rooftop solar PV system. Solar Energy 216, 518–529. https://doi.org/10.1016/j.solener.2021.01.045
5. Bhuvad, S.S., Udayraj, 2022. Investigation of annual performance of a building shaded by rooftop PV panels in different climate zones of India. Renewable Energy 189, 1337–1357. https://doi.org/10.1016/j.renene.2022.03.004
6. Central Electricity Authority (CEA), 2024. CO_2 Baseline Database for the Indian Power Sector: User Guide Version 19.0. Government of India, Ministry of Power, New Delhi.
7. Chaturvedi, S., Elangovan, R., 2023. Grey Wolf algorithmic framework for building energy optimization in India's Köppen–Geiger climatic zones. Advances in Building Energy Research 17 (3), 277–302. https://doi.org/10.1080/17512549.2023.2184422

8. Chaturvedi, S., Rajasekar, E., 2022. Application of a probabilistic LHS-PAWN approach to assess building cooling energy demand uncertainties. Building Simulation 15 (3), 373–387. https://doi.org/10.1007/s12273-021-0815-6
9. Chaturvedi, S., Rajasekar, E., Natarajan, S., 2020. Multi-objective building design optimization under operational uncertainties using the NSGA II algorithm. Buildings 10 (5), 88. https://doi.org/10.3390/buildings10050088
10. Choi, S., Ishii, T., Sato, R., Chiba, Y., Masuda, A., 2018. Performance degradation due to outdoor exposure and seasonal variation in amorphous silicon photovoltaic modules. Thin Solid Films 661, 116–121. https://doi.org/10.1016/j.tsf.2018.07.017
11. Coppitters, D., De Paepe, W., Contino, F., 2019. Surrogate-assisted robust design optimization and global sensitivity analysis of a directly coupled photovoltaic-electrolyzer system under techno-economic uncertainty. Applied Energy 248, 310–320. https://doi.org/10.1016/j.apenergy.2019.04.101
12. Crawley, D.B., Lawrie, L.K., Winkelmann, F.C., Buhl, W.F., Huang, Y.J., Pedersen, C.O., Strand, R.K., Liesen, R.J., Fisher, D.E., Witte, M.J., Glazer, J., 2001. EnergyPlus: creating a new-generation building energy simulation program. Energy and Buildings 33 (4), 319–331. https://doi.org/10.1016/S0378-7788(00)00114-6
13. De Soto, W., Klein, S.A., Beckman, W.A., 2006. Improvement and validation of a model for photovoltaic array performance. Solar Energy 80 (1), 78–88. https://doi.org/10.1016/j.solener.2005.06.010
14. Delgarm, N., Sajadi, B., Kowsary, F., Delgarm, S., 2016. Multi-objective optimization of the building energy performance: A simulation-based approach by means of particle swarm optimization (PSO). Applied Energy 170, 293–303. https://doi.org/10.1016/j.apenergy.2016.02.141
15. Dominguez, A., Kleissl, J., Luvall, J.C., 2011. Effects of solar photovoltaic panels on roof heat transfer. Solar Energy 85 (9), 2244–2255. https://doi.org/10.1016/j.solener.2011.06.010
16. Duffie, J.A., Beckman, W.A., 2013. Solar Engineering of Thermal Processes, 4th ed. John Wiley & Sons, Hoboken, NJ.
17. Eon, C., Breadsell, J.K., Byrne, J., Morrison, G.M., 2020. The discrepancy between as-built and as-designed in energy efficient buildings: A rapid review. Sustainability 12 (16), 6372. https://doi.org/10.3390/su12166372
18. Gujarat Electricity Regulatory Commission (GERC), 2016. Gujarat Electricity Regulatory Commission (Net Metering Rooftop Solar PV Grid Interactive Systems) Regulations, 2016. Notification No. 5/2016, dated 18 June 2016, as amended. GERC, Gandhinagar.
19. Harkouss, F., Fardoun, F., Biwole, P.H., 2018. Passive design optimization of low energy buildings in different climates. Energy 165, 591–613. https://doi.org/10.1016/j.energy.2018.09.019
20. Hoseinzadeh, P., Khalaji Assadi, M., Heidari, S., Khalatbari, M., Saidur, R., Haghighat nejad, K., Sangin, H., 2021. Energy performance of building integrated photovoltaic high-rise building: Case study, Tehran, Iran. Energy and Buildings 235, 110707. https://doi.org/10.1016/j.enbuild.2020.110707
21. International Electrotechnical Commission (IEC), 2021. IEC 61724-1:2021 Photovoltaic system performance – Part 1: Monitoring, 2nd ed. IEC, Geneva.
22. Jordan, D.C., Kurtz, S.R., 2013. Photovoltaic degradation rates — an analytical review. Progress in Photovoltaics: Research and Applications 21 (1), 12–29. https://doi.org/10.1002/pip.1182
23. Joshi, K.A., Pindoriya, N.M., 2012. Impact investigation of rooftop solar PV system: A case study in India. In: 2012 3rd IEEE PES Innovative Smart Grid Technologies Europe (ISGT Europe), Berlin, pp. 1–8. https://doi.org/10.1109/ISGTEurope.2012.6465813
24. Kapsalis, V., Karamanis, D., 2015. On the effect of roof added photovoltaics on building's energy demand. Energy and Buildings 108, 195–204. https://doi.org/10.1016/j.enbuild.2015.09.016
25. Kapsalis, V.C., Vardoulakis, E., Karamanis, D., 2014. Simulation of the cooling effect of the roof-added photovoltaic panels. Advances in Building Energy Research 8 (1), 41–54. https://doi.org/10.1080/17512549.2014.890534
26. Kotireddy, R., Hoes, P.-J., Hensen, J.L.M., 2019. Integrating robustness indicators into multi-objective optimization to find robust optimal low-energy building designs. Journal of Building Performance Simulation 12 (5), 546–565. https://doi.org/10.1080/19401493.2018.1526971
27. Kumar, P., Gupta, S., Dagar, V., 2024. Sustainable energy development through non-residential rooftop solar photovoltaic adoption: Empirical evidence from India. Sustainable Development 32 (1), 795–814. https://doi.org/10.1002/sd.2644
28. Li, H., Zhang, J., Liu, X., Zhang, T., 2022. Comparative investigation of energy-saving potential and technical economy of rooftop radiative cooling and photovoltaic systems. Applied Energy 328, 120181. https://doi.org/10.1016/j.apenergy.2022.120181

29. Liu, S., Kwok, Y.T., Lau, K.K.-L., Tong, H.W., Chan, P.W., Ng, E., 2020. Development and application of future design weather data for evaluating the building thermal-energy performance in subtropical Hong Kong. Energy and Buildings 209, 109696. https://doi.org/10.1016/j.enbuild.2019.109696
30. Luthander, R., Widén, J., Nilsson, D., Palm, J., 2015. Photovoltaic self-consumption in buildings: A review. Applied Energy 142, 80–94. https://doi.org/10.1016/j.apenergy.2014.12.028
31. Ma, Z., Hu, L., Mao, H., Shao, Q., Tian, Z., Luo, Y., Deng, J., Sun, D., Fan, J., 2023. Shading effect and energy-saving potential of rooftop photovoltaic on the top-floor room. Solar Energy 265, 112099. https://doi.org/10.1016/j.solener.2023.112099
32. Malvoni, M., Kumar, N.M., Chopra, S.S., Hatziargyriou, N., 2020. Performance and degradation assessment of large-scale grid-connected solar photovoltaic power plant in tropical semi-arid environment of India. Solar Energy 203, 101–113. https://doi.org/10.1016/j.solener.2020.04.011
33. Ministry of New and Renewable Energy (MNRE), 2024. PM Surya Ghar: Muft Bijli Yojana. Scheme guidelines and benchmark costs for residential rooftop solar, effective 13 February 2024. Government of India, New Delhi.
34. Odeh, S., Pearling, L., 2025. Experimental work to investigate the effect of rooftop PV panel shading on building thermal performance. Energies 18 (13), 3429. https://doi.org/10.3390/en18133429
35. Pramadya, F.A., Kim, K.N., 2024. Promoting residential rooftop solar photovoltaics in Indonesia: Net-metering or installation incentives? Renewable Energy 222, 119901. https://doi.org/10.1016/j.renene.2023.119901
36. Ramapragada, P., Tejaswini, D., Garg, V., Mathur, J., Gupta, R., 2022. Investigation on air conditioning load patterns and electricity consumption of typical residential buildings in tropical wet and dry climate in India. Energy Informatics 5 (S4), 61. https://doi.org/10.1186/s42162-022-00228-1
37. Ren, H., Sun, Y., Tse, C.F.N., Fan, C., 2023. Optimal packing and planning for large-scale distributed rooftop photovoltaic systems under complex shading effects and rooftop availabilities. Energy 274, 127280. https://doi.org/10.1016/j.energy.2023.127280
38. Saez, R., Boer, D., Shobo, A.B., Vallès, M., 2024. Self-consumption potential and surplus compensation policy impact on rooftop photovoltaic systems in Spain. Renewable Energy 229, 120713. https://doi.org/10.1016/j.renene.2024.120713
39. Saltelli, A., Annoni, P., Azzini, I., Campolongo, F., Ratto, M., Tarantola, S., 2010. Variance based sensitivity analysis of model output. Design and estimator for the total sensitivity index. Computer Physics Communications 181 (2), 259–270. https://doi.org/10.1016/j.cpc.2009.09.018
40. Sharma, P., Bojja, H., Yemula, P., 2016. Techno-economic analysis of off-grid rooftop solar PV system. In: 2016 IEEE 6th International Conference on Power Systems (ICPS), New Delhi. https://doi.org/10.1109/ICPES.2016.7584208
41. Sharma, Y., Saxena, B.K., Mishra, S., 2019. Techno-economic analysis of rooftop solar PV system by variation in PV module capacity. In: 2019 2nd International Conference on Power and Embedded Drive Control (ICPEDC), Chennai, pp. 355–360. https://doi.org/10.1109/ICPEDC47771.2019.9036479
42. Sherman, P., Lin, H., McElroy, M., 2022. Projected global demand for air conditioning associated with extreme heat and implications for electricity grids in poorer countries. Energy and Buildings 268, 112198. https://doi.org/10.1016/j.enbuild.2022.112198
43. Sherwani, A.F., Usmani, J.A., Varun, 2010. Life cycle assessment of solar PV based electricity generation systems: A review. Renewable and Sustainable Energy Reviews 14 (1), 540–544. https://doi.org/10.1016/j.rser.2009.08.003
44. Shi, X., Tian, Z., Chen, W., Si, B., Jin, X., 2016. A review on building energy efficient design optimization from the perspective of architects. Renewable and Sustainable Energy Reviews 65, 872–884. https://doi.org/10.1016/j.rser.2016.07.050
45. Shukla, A.K., Sudhakar, K., Baredar, P., 2016. Design, simulation and economic analysis of standalone rooftop solar PV system in India. Solar Energy 136, 437–449. https://doi.org/10.1016/j.solener.2016.07.009
46. United Nations Environment Programme (UNEP), 2025. Global Status Report for Buildings and Construction 2024/2025: Not Just Another Brick in the Wall. UNEP, Nairobi.
47. Wang, D., Qi, T., Liu, Y., Wang, Y., Fan, J., Wang, Y., Du, H., 2020. A method for evaluating both shading and power generation effects of rooftop solar PV panels for different climate zones of China. Solar Energy 205, 432–445. https://doi.org/10.1016/j.solener.2020.05.009
48. Zheng, Y., Weng, Q., 2020. Modeling the effect of green roof systems and photovoltaic panels for building energy savings to mitigate climate change. Remote Sensing 12 (15), 2402. https://doi.org/10.3390/rs12152402